Journal of the Korean Physical Society (2022) 81:1020–1028
https://doi.org/10.1007/s40042-022-00575-y

Online ISSN 1976-8524
Print ISSN 0374-4884

ORIGINAL PAPER - CROSS-DISCIPLINARY PHYSICS AND RELATED AREAS OF SCIENCE AND TECHNOLOGY

Feasibility of a method for optimizing the electrode array structure in tumor-treating fields therapy

Geon Oh[1] · Yongha Gi[1] · Heehun Sung[1] · Hyunwoo Kim[1] · Jaehyeon Seo[1] · Myonggeun Yoon[1,2] · Yunhui Jo[3]

Received: 25 October 2021 / Revised: 30 December 2021 / Accepted: 17 January 2022 / Published online: 8 August 2022

Abstract
The present study investigated electrode array structures that maximize the therapeutic electric field intensity to tumors with different shapes and locations, while minimizing electric field intensity to the surrounding organs at risk (OARs). A human body phantom model was created from magnetic resonance images of a patient and divided into regions including a tumor and OARs. The shapes and sizes of the electrode arrays were altered for tumors differing in shape and location, and these electrode array structures were tested in the phantom. Use of a conformal electrode array based on the shape of the tumor maintained therapeutic electric field intensity to the tumor while reducing electric field intensity to the surrounding OARs by approximately 18%. Although the electric field intensity delivered to the tumor was proportional to the size of the electrode array, it was saturated at a critical area. Simulation results showed that optimal sizes of electrode arrays for specific tumors located at depths of 2 cm, 4 cm and 6 cm were 91, 273 and 830 cm^2, respectively, indicating that the optimal size of the electrode array is proportional to the depth of tumor in the phantom. These results suggest that a tumor location-dependent optimal ratio between the size of the electrode array and the size of the individual electrodes could be calculated. In summary, this study indicated that customizing the electrode array structure to individual tumors can markedly increase the electric field intensity delivered to the tumor while minimizing the intensity delivered to OARs.

Keywords Tumor-treating fields · Electric field intensity · Tumor · Organ at risk · Phantom · Electrode array

1 Introduction

Cancer is the leading cause of human death, making it a major public health problem [1]. Certain cancers are refractory to traditional methods, such as surgery, chemotherapy and radiotherapy, making it necessary to develop alternative but effective cancer treatment methods. Tumor-treating fields (TTFs) therapy is emerging as a promising cancer treatment method, because it selectively kills dividing cancer cells and has little effect on normal non-dividing cells [2–4].

The ability of TTFs therapy to inhibit cancer cell proliferation is dependent on the magnitude of the electric field transmitted to the cancer cells. Specifically, a greater electric field is associated with a greater inhibition of cell proliferation [4–6]. This tendency has been demonstrated in vitro [4] and in a clinical trial in 340 patients with brain tumors [7]. Moreover, the latter study showed that the power loss density in TTFs therapy, which is proportional to the square of the electric field magnitude, is correlated with its effectiveness [7]. In that study, the median overall survival (OS) was found to be 4.8 months longer in patients subjected to TTFs therapy of power loss density ≥ 0.77 mW/cm^3 in the tumor compared to those with a power loss density of < 0.77 mW/cm^3, providing theoretical support for the importance of the electric field in clinical practice.

The electrodes used in clinical practice for electric field therapy are part of an array. Currently, the electrode arrays have set shapes and sizes independent of the tumor or region of interest within a patient's body [8]. Thus, the electric field may not be focused to the tumor or may affect

✉ Myonggeun Yoon
radioyoon@korea.ac.kr

[1] Department of Bioengineering, Korea University, Seoul 02841, Republic of Korea

[2] FieldCure Ltd, Seoul 02481, Republic of Korea

[3] Institute of Global Health Technology, Korea University, Seoul 02841, Republic of Korea

the surrounding organs at risk (OARs). Patients undergoing electric field therapy using such electrode arrays may, therefore, experience side effects that limit the effectiveness of treatment [9]. However, the effectiveness and safety of treatment may be enhanced by using an optimized electrode array structure that maximizes the electric field to the tumor, while minimizing the field applied to OARs. Such optimization would result in better clinical outcomes than current treatment methods.

The present study evaluated simulations of an electric field delivered to tumors based on their size, shape, and depth within a human body. Simulations were performed by varying the shape and total size of the electrode array, the size and shape of the individual electrodes constituting the array, and the ratio between the area occupied by individual electrodes and the total area of the electrode array. These simulation results suggested a method for determining the optimized electrode array that maximizes the electric field transmitted to the tumor while minimizing the electric field transmitted to surrounding OARs.

2 Materials and methods

2.1 Method for optimizing electrode array structure

Electrotherapy using an electrode array customized for a particular tumor consists of multiple stages. First, the segmentation stage imports 3D medical image data from a patient's medical images and segments the tumor and the OARs. Second, the overall shape of the electrode array is determined by how the array is attached such that it conforms to the shape of the tumor. Third, the electrode array size is optimized to maximize the average magnitude of the electric field transmitted to the tumor. Fourth, the ratio of the sum of the sizes of the individual electrodes and the total size of the electrode array, called the area ratio, is optimized to maximize the electric field to the tumor. Specifically, this optimization is performed by determining the correlation of the area ratio with the magnitude of the electric field transmitted to the tumor. Finally, electric field therapy is simulated using the patient-customized electrode array resulting from these processes (Fig. 1).

2.2 Creating the simulation model

A customized model was created from a patient's imaging data obtained from an open-source DICOM file of clinical magnetic resonance images (Fig. 2a). The OARs (i.e., the liver, lungs, and spleen) and the virtual tumor in the images were segmented using the Mimics® Innovation Suite 23 (Materialise NV, Belgium). The masks that marked imaging data slice-by-slice in Mimics were created (Fig. 2b), and the desired 3D object was created based on the masks (Fig. 2c). A human body model was created with the image objects using COMSOL Multiphysics (COMSOL Inc., Sweden) software, and this model was used to fabricate a humanoid phantom. The tumor and

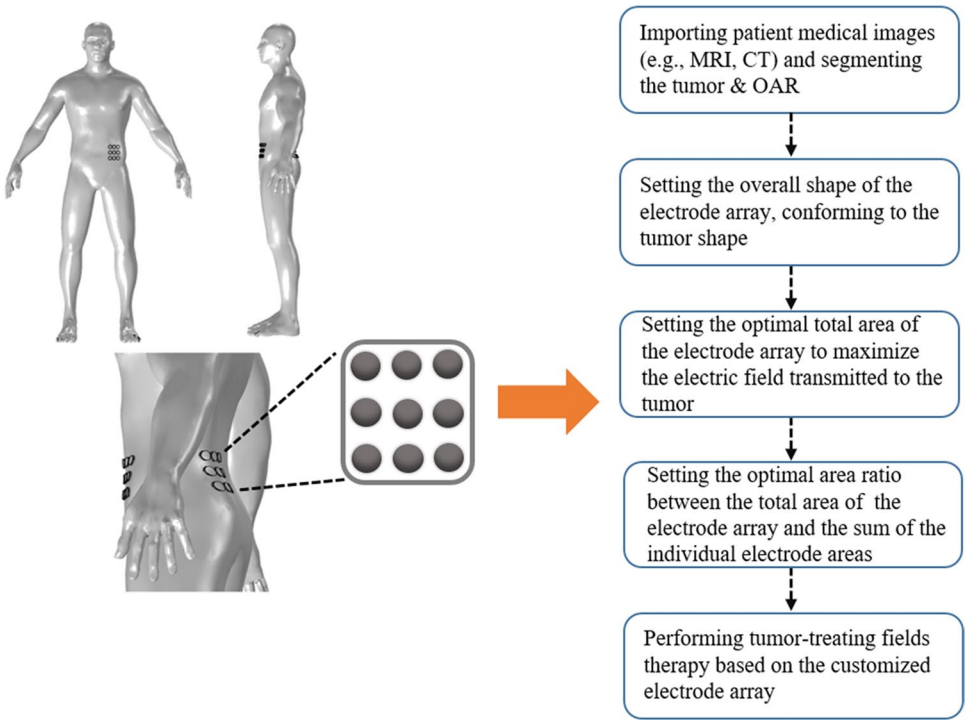

Fig. 1 Electrode pads and attachments currently used for TTFs therapy in clinical practice (left) and a flowchart showing the method used in this study to optimize electrode array structures in TTFs therapy (right)

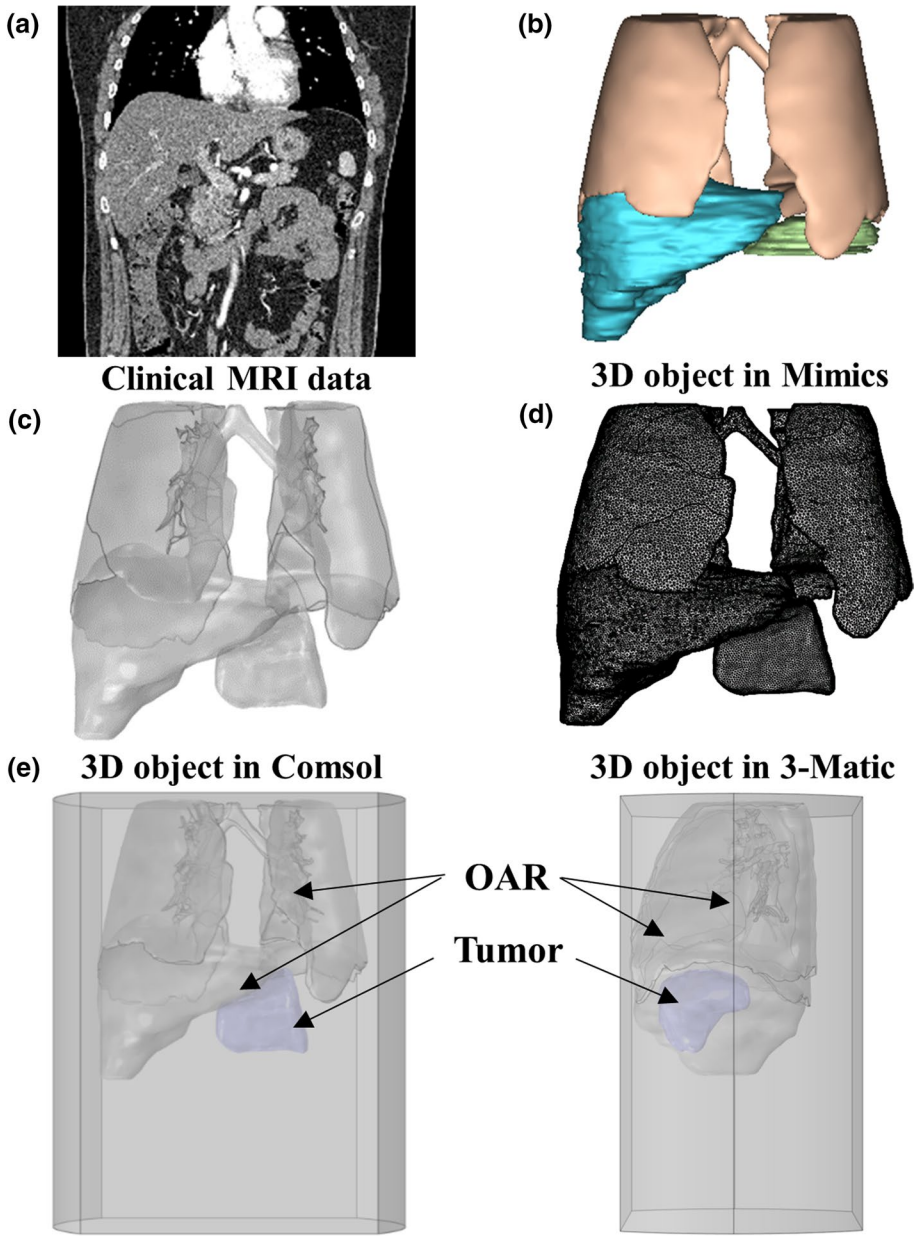

Fig. 2 **a** Clinical MRI data used in the simulation. **b** Creation of a mask and an object from clinical MRI data in Mimics software. **c** Importation into the COMSOL Multiphysics software program to create a human body model. **d** Creation of a mesh in the 3-Matic program and its analysis in COMSOL Multiphysics. **e** Mesh structure of the final model for analysis in COMSOL Multiphysics

OARs in the phantom were also created and positioned. The fabricated electrode array was attached to the humanoid phantom, and soft mesh structures for all objects were created using 3-Matic modeling software (Materialise NV) (Fig. 2d). These structures were merged with the mesh structure to generate the final model for analysis using COMSOL Multiphysics software (Fig. 2e).

2.3 Solving the simulation model

The distribution and magnitude of the electric field in the experimental model were analyzed in the electric currents interface of COMSOL Multiphysics. Specifically, electric field analysis was performed using a quasi-static approximation of Maxwell's equations:

$$\mathrm{J} = \sigma \mathrm{E} + \frac{\partial D}{\partial t} + J_e \tag{1}$$

$$\nabla \bullet \mathrm{J} = Q_{j,v} \tag{2}$$

$$\mathrm{E} = -\nabla \mathrm{V}, \tag{3}$$

where J = current density (A/m^2), σ = electrical conductivity (S/m), E = electric field intensity (V/m), ∂D/∂t = change in electric displacement field over time (C/m^2), $Q_{j,v}$ = electric

charge (C), and V = electric potential (V). Equation (1) shows that the total current density is the sum of the displacement current density, the external current density, and the electric field intensity multiplied by the electrical conductivity. Equation (2) shows the conservation of charge, and Eq. (3) shows that the electric field intensity equals the negative of the gradient of the electric potential [10, 11].

Table 1 Electric properties of various tissues and electrodes at 150 kHz

Object	Conductivity, σ (s/m)	Relative permittivity,ε_r
Body		
Lung	0.11	1980
Liver	0.095	6090
Spleen	0.12	3740
Tissue	0.3	8000
Tumor	0.25	4000
Elctrode		
Metal	5.998e7	1
Ceramic insulator	0	10,000
Hydrogel	0.1	100

The simulations were performed by adjusting the magnitude of the electric field so that the current density on the skin surface of the humanoid phantom would be less than the allowable current density of about 35 mA/cm^2 while applying an electric field as a sine waveform with a frequency of 150 kHz [4]. Thus, all the materials within the model were designed to have electric properties of human body tissues in an electric field with a frequency of 150 kHz (Table 1).

3 Results

Figure 3 shows the electric field distributions for electric field therapy applied to a hypothetical tumor and OARs in the human body model when using a simple rectangular electrode (Fig. 3a) and when using an electrode structure tailored to the shapes of the tumor and the OARs (Fig. 3c). This simulation result showed that the average magnitudes of the electric field applied to the tumor and OARs (per volume) were 3.06 V/cm and 2.27 V/cm, respectively, when using an electrode that did not consider the shapes of the tumor and the OARs (Fig. 3b)). When the electric field was applied using electrodes that considered the shapes of the tumor and the OARs in the model, the average magnitudes

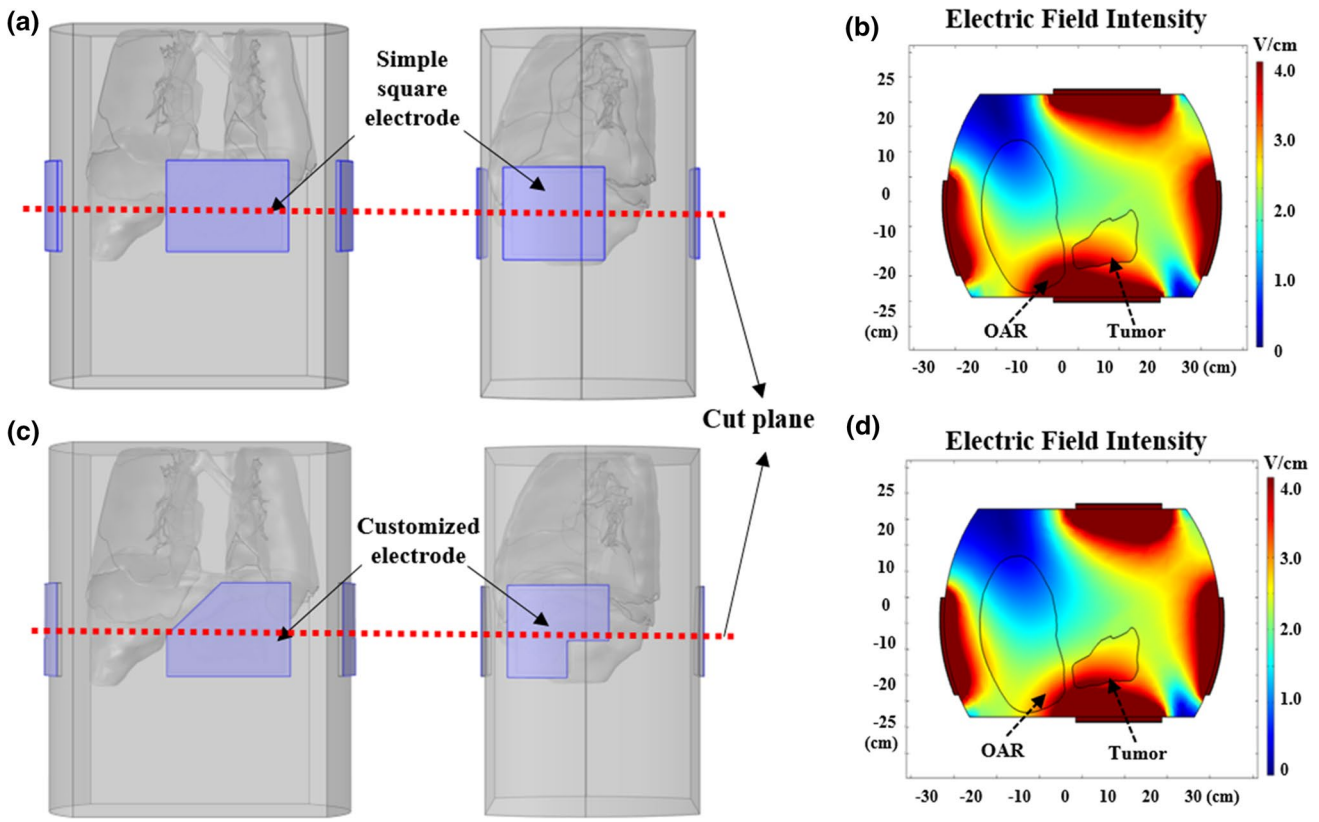

Fig. 3 Methods of applying the electric field and the distribution of the electric field on the cutting plane using (**a**, **b**) a simple rectangular electrode without considering the shape of the tumor and (**c**, **d**) a customized electrode considering the shape of the tumor

of the applied electric field, per volume, were 3.06 V/cm and 1.87 V/cm for the tumor and OARs, respectively (Fig. 3d). The relative electric field intensity delivered to the OARs was reduced by ~ 18%, from 2.27 to 1.87 V/cm, whereas the relative electric field intensity delivered to the tumor was the same.

Figure 4 shows the correlation between the total electrode size (or area) and the average magnitude of the electric field transmitted to the tumor per unit volume. The total electrode sizes in the simulation were 60, 153, 238, 402, 534, 769, and 948 cm^2, and the average electric field magnitudes per unit volume transmitted from the electrode area to the tumor were 1.9, 2.8, 3.14, 3.58, 3.71, 3.81, and 3.82 V/cm, respectively (Fig. 4). The average electric field magnitude per volume became saturated around total electrode areas of 700–800 cm^2, corresponding to the approximate value of the saturated critical area (SCA) (Fig. 4b). SCA can be calculated using the equation:

$$\begin{aligned}&(\text{Saturation critical area}\\&= \left(\text{the minimum value of A satisfying} \frac{dE}{dA} \cong 0\right),\end{aligned} \tag{4}$$

where E is the average magnitude of the electric field transmitted to the tumor and A is the total electrode area.

Figure 5 shows the correlation between total electrode size and the average magnitude of the electric field transmitted to the tumor, as a function of the voltage applied to different tumor depths within the body. The distances from the electrode to the tumor were 2 cm, 4 cm, and 6 cm. The graph in Fig. 5b is similar to that in Fig. 4b for various depths of tumor inside phantom. The measured SCAs for distances of 2 cm, 4 cm, and 6 cm were 91 cm^2, 273 cm^2, and 830 cm^2, respectively.

Figure 6a, b shows the difference between using a single-plate electrode and an electrode array on a curved part of the patient's body. Specifically, although many empty spaces not covered by the planar electrode were visible when a large-area, single-plate electrode was attached to the curved body part, few spaces were observed when a three-electrode array was attached to the same curved body part.

Figure 7a shows an example of the total size (or area) of an electrode array and the size (or area) of constituent individual electrodes. In determining the therapeutic electric field delivered to the tumor, the sum of the areas of the individual electrodes should be reduced, because a reduction in electrode area would reduce current to the skin, resulting in fewer side effects. The optimal ratio of the sum of the areas covered by all individual electrodes to the total area covered by the electrode array was determined by assessing the relationship between this ratio and the magnitude of the electric field transmitted to the tumor (Fig. 7b). A lower ratio was found to be associated with a reduced average electric field magnitude transmitted to the tumor. When

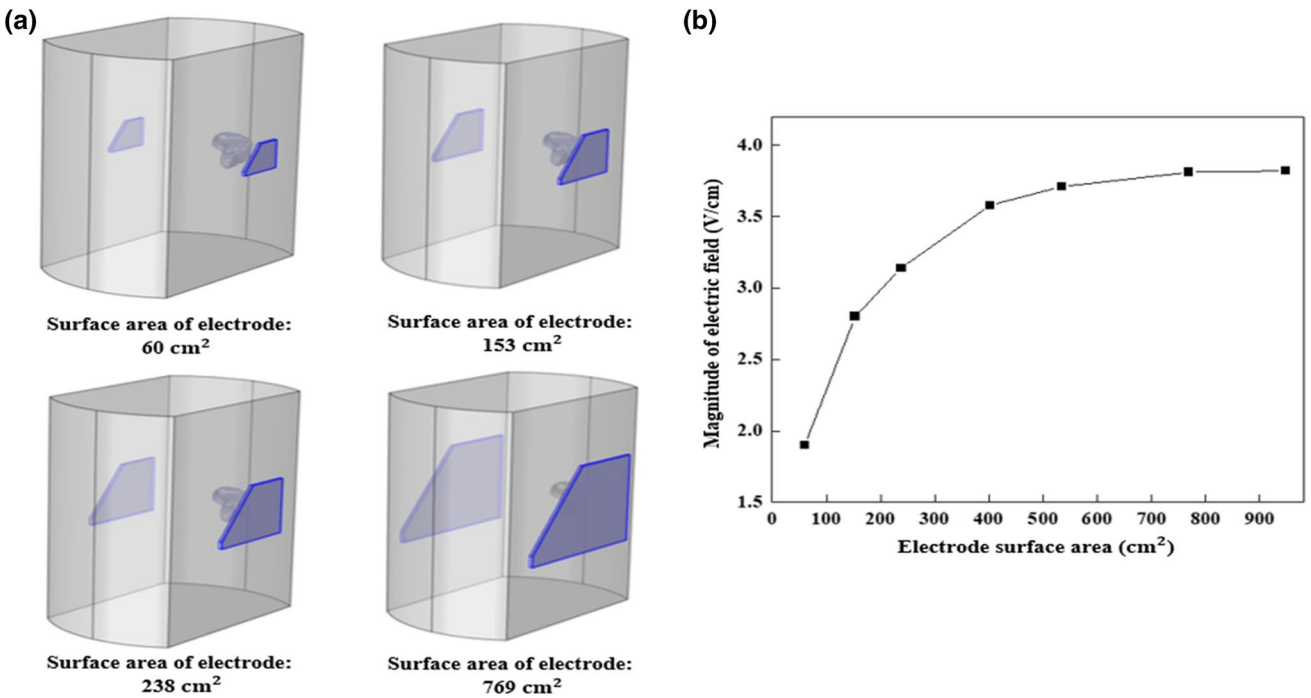

Fig. 4 Correlation between the total area of an electrode and the average magnitude of an electric field transmitted to a tumor when a voltage was applied. **a** Example of attaching conformal electrodes corresponding to the tumor shape but having different total areas. **b** Graph showing the correlation between the total area of the electrode and the average magnitude of the electric field delivered to the tumor

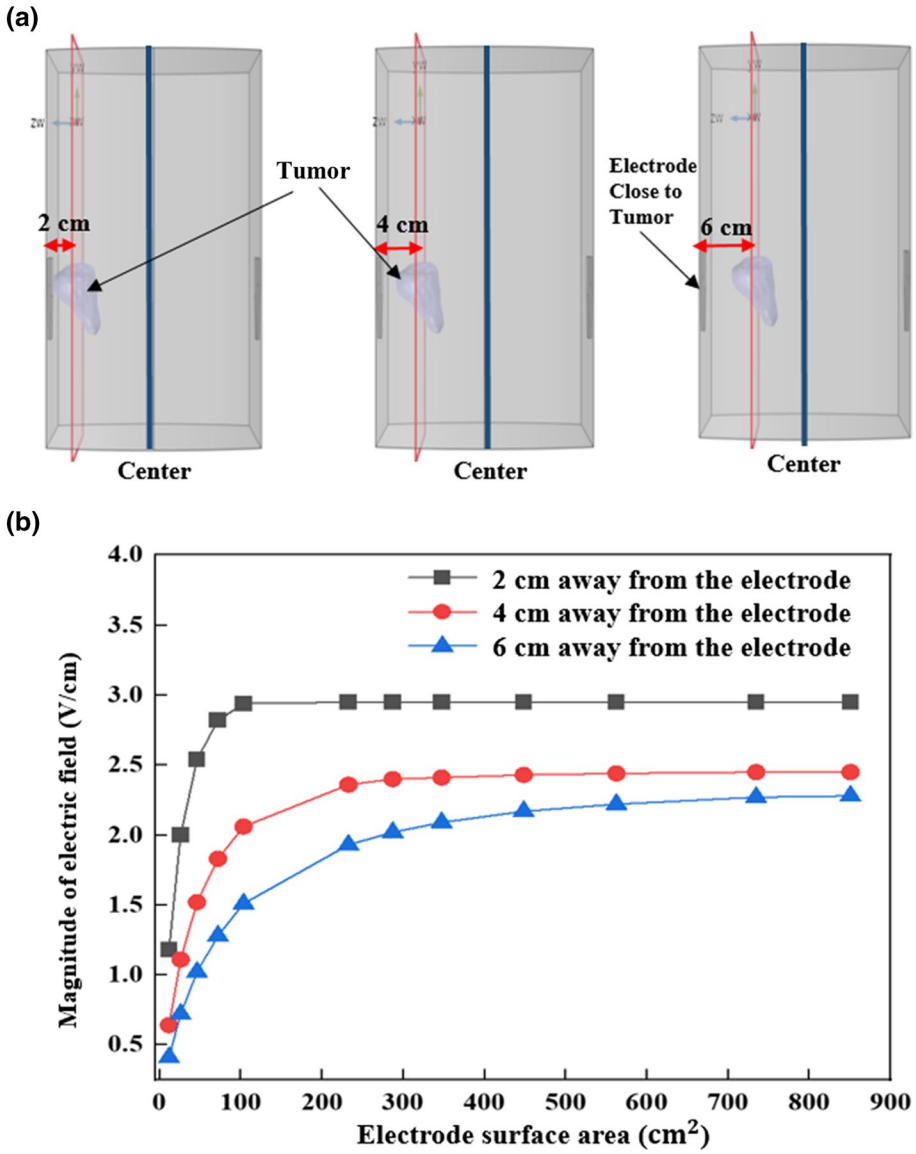

Fig. 5 Correlation between the total area of the electrode and the average magnitude of the electric field transmitted to the tumor subject to the applied voltage for different depths of the tumor within the body. **a** State in which the distance between the ROI from the electrode are 2 cm, 4 cm, and 6 cm. **b** Graph showing that the SCAs for distances of 2 cm, 4 cm, 6 cm were 91 cm^2, 273 cm^2, 830 cm^2, respectively

the shape, size, and position of the tumor were fixed, the magnitude of the electric field could be adjusted by varying the areas of the individual electrodes within the total area of the electrode array as well by varying the areas of empty spaces between the electrodes. If the therapeutic magnitude of the electric field to the tumor was set at 1 V/cm, the optimal ratio of the individual electrodes to electrode array was approximately ± 32%, as shown by the dotted line in Fig. 7b.

4 Discusssion

This study retrieved information about a tumor, including its location, shape, and size, as well as OARs, from MRI data of individual patients undergoing electric field therapy. Based on information about the tumor and OARs in individual patients, the method proposed in this study would maximize the efficacy of electric field therapy using an electrode array customized for each patient.

The average magnitude of an optimized electric field transmitted to the tumor and OARs was shown to be altered by changes in the shape and area of the electrode array attached to the body. The average magnitude of the electric field transmitted to the tumor by a total electrode array was found to increase in proportion to the total electrode area. In addition, a saturation zone was observed, defined as an area over which the electric field magnitude in the tumor became constant. The saturation critical area, or SCA, was the area in which this magnitude began to become saturated. The SCA was found to depend on the distance between the tumor and the electrode. Thus, the shape, size, and location of the tumor relative to the electrode attachment should be considered when configuring an optimized electrode array for efficient electric field therapy.

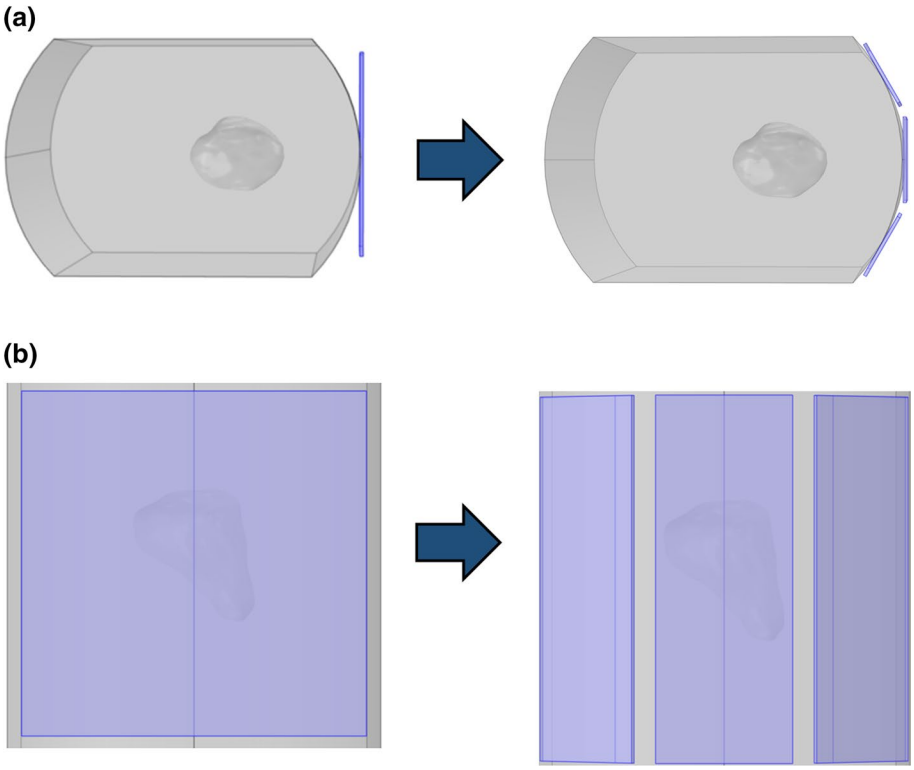

Fig. 6 Electric field therapy with (**a**, **b**) a single-plate electrode and an electrode array consisting of several individual electrodes attached to a curved part of a patient's body

Additionally, the present findings illustrate a method for configuring individual electrodes within the overall shape and area of a pre-determined electrode array. When the shape, size, and position of the tumor are fixed, the ratio of the individual electrode area to the total array area should be set by adjusting the areas of both the individual electrodes and the empty spaces between electrodes. Applying these methods can optimize the electrode array configuration, which in turn maximizes the magnitude of the electric field to the tumor while also minimizing the electric field to the OARs.

Although an algorithmic method that adjusts the voltage levels of individual electrodes can optimize electric field treatment [12, 13], that approach has drawbacks in clinical practice. Electrode arrays in clinical practice [9] contain more than 70 individual electrodes, with identical voltage applied to each electrode within the array. Therefore, the aforementioned optimization methods require that the magnitude of the applied voltage be adjusted independently for the more than 70 included electrodes. The development of such an individualized control device would involve complex hardware design. Additionally, patients would have to be responsible for increased costs related to the use of this device.

Furthermore, when optimizing the voltage applied to each electrode, it is not safe to apply a voltage exceeding the allowed current density (i.e., the maximum current density that causes no harm to the human body). Thus, the ability to increase the magnitude of the electric field transmitted to the tumor is limited. In contrast, the method proposed here (i.e., optimizing electric field therapy by changing the electrode configuration) is simpler and more practical than the algorithmic method [12, 13]. Specifically, the proposed method can maximize the magnitude of the electric field transmitted to the tumor without having to apply voltages of different magnitudes to individual electrodes. At the same time, it can minimize the magnitude of the electric field transmitted to the OARs.

Further research is necessary, however, to resolve the problems associated with over-simplification in optimizing the electrode array configuration. A human body undergoing electric field therapy is subject to a variety of conditions that are far more complex than the conditions used in this study. For example, tissues within the same organ may have different properties, whereas our model assumes uniform soft tissue. Therefore, to obtain more accurate simulation results, it is necessary to subdivide regions of the body and assign properties to each. Moreover, the inclusion in Eqs. 1, 2, 3 of variables and factors based on the biological environment within the human body would provide more accurate calculations.

Lastly, more in-depth studies are required to optimize the electrode array configuration. Artificial intelligence (AI) technologies may be a good candidate for optimization of these configurations. Deep learning-based AI technologies are currently used in various research fields, including

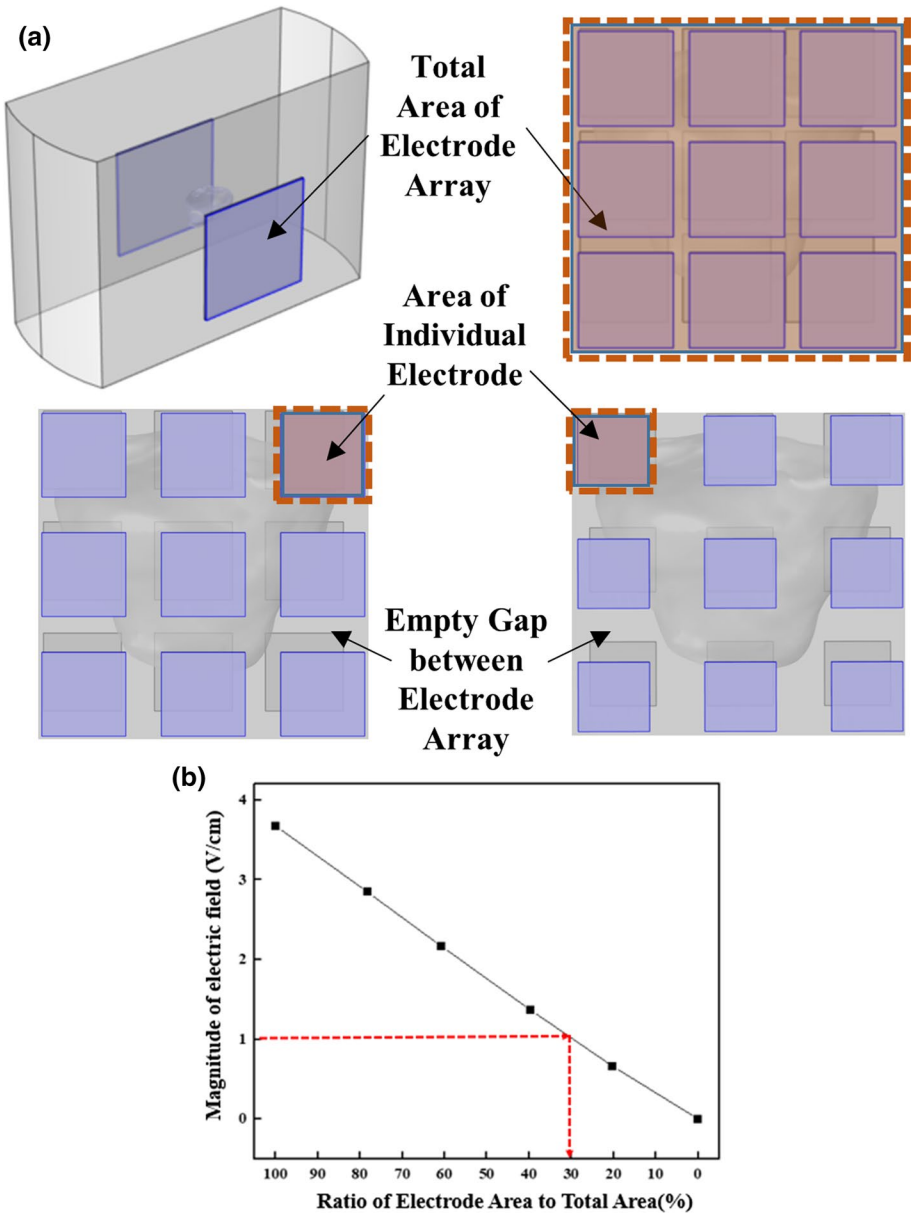

Fig. 7 Ratios of the sum of the areas covered by individual electrodes and the total area of the electrode array with the magnitude of the electric field transmitted to the tumor for an electrode array of fixed total area. **a** Example showing the total area of the electrode array, the area of individual electrodes and the area of empty gap between electrodes. **b** Correlation between the average magnitude of the electric field transmitted to the tumor and the area ratio

medicine. AI technology could be harnessed in our proposed electrode array optimization method, enabling the electrode array to be automatically configured, thereby improving the efficiency of electric field therapy.

5 Conclusion

This study describes a method for customizing the configuration of electrode arrays for optimal electric field therapy. This customization is based on the shape, size, and location of the tumor. This method, in which the overall shape, area, and configuration of individual electrodes in an electrode array were altered, was shown to maximize the magnitude of the electric field transmitted to the tumor while minimizing the electric field transmitted to surrounding OARs. These findings may lead to the development of electric field therapy with improved efficacy and may also open up possibilities for novel electric field therapy methods.

Acknowledgements This work was supported by a Korea Medical Device Development Fund grant funded by the government of Korea (the Ministry of Science and ICT, the Ministry of Trade, Industry and Energy, the Ministry of Health & Welfare, and the Ministry of Food and Drug Safety) (Project Number: 202012E01); by a National Research Foundation of Korea (NRF) grant funded by the Korea government (MSIT) (2021R1A2C2008695) (2022R1A2C1010337); and by a Korea University Grant.

References

1. F. Bray, J. Ferlay, I. Soerjomataram, R.L. Siegel, L.A. Torre, A. Jemal, CA: A Cancer Journal Clin (2018). https://doi.org/10.3322/caac.21492
2. A.M. Davies, U. Weinberg, Y. Palti, Ann N Y Acad Sci **1291**, 86 (2013)
3. E.D. Kirson, Z. Gurvich, R. Schneiderman, E. Dekel, A. Itzhaki, Y. Wasserman, R. Schatzberger, Y. Palti, Can Res **64**, 3288 (2004)
4. E.D. Kirson, V. Dbalý, F. Tovaryš, J. Vymazal, J.F. Soustiel, A. Itzhaki, D. Mordechovich, S. Steinberg-Shapira, Z. Gurvich, R. Schneiderman, Proc Natl Acad Sci **104**, 10152 (2007)
5. Y. Jo, J. Sung, H. Jeong, S. Hong, Y.K. Jeong, E.H. Kim, M. Yoon, Technol Cancer Res Treat **18**, 1533033819845008 (2019)
6. E.H. Kim, H.S. Song, S.H. Yoo, M. Yoon, Oncotarget **7**, 65125 (2016)
7. M.T. Ballo, N. Urman, G. Lavy-Shahaf, J. Grewal, Z.E. Bomzon, S. Toms, Int J Radiat Oncol Biol Phys (2019). https://doi.org/10.1016/j.ijrobp.2019.04.008
8. D. Fabian, M.D.P. Guillermo Prieto Eibl, I. Alnahhas, N. Sebastian, P. Giglio, V. Puduvalli, J. Gonzalez, J.D. Palmer, Cancers (2019). https://doi.org/10.3390/cancers11020174
9. F. Rivera, M. Benavides, J. Gallego, C. Guillen-Ponce, J. Lopez-Martin, M. Küng, Pancreatology **19**, 64 (2019)
10. F. Assous, P. Degond, E. Heintze, P.-A. Raviart, J. Segré, J Comput Phys **109**, 222 (1993)
11. K.T. Selvan, IEEE Antennas Propag Mag **51**, 36 (2009)
12. J. Sung, J. Seo, Y. Jo, M. Yoon, S.-G. Hwang, E.H. Kim, J Korean Phys Soc **73**, 1577 (2018). https://doi.org/10.3938/jkps.73.1577
13. Z. Bomzon, N. Urman, H.S. Hershkovich, E.D. Kirson, A. Naveh, R. Shamir, E. Federov, C. Wenger, U. Weinberg, Am Soc Clin Oncol (2019)